Experimental Results on the Effect of Surface Structures on the Flame Propagation Velocity of PMMA in Microgravity

Experimental Results on the Effect of Surface Structures on the Flame Propagation Velocity of PMMA in Microgravity

Christian Eigenbrod[1], Jakob Hauschildt[2], Florian Meyer[2]
ZARM, University of Bremen, 28359 Bremen, Germany

David L. Urban[3], Gary A. Ruff[4], Sandra L. Olson[5]
NASA Glenn Research Center, Cleveland, OH, USA

Paul V. Ferkul[6]
USRA, Cleveland, OH, USA

Grunde Jomaas[7]
BRE Centre for Fire Safety Engineering, University of Edinburgh, UK

and

Balazs Toth[8]
ESA-ESTEC, Noordwijk, The Netherlands

Materials foreseen for the design of manned spacecraft must pass the NASA-STD 6001B Test 1 regarding its fire hazard. During this qualification test in 1g conditions, a flat sample with fire protected edges is placed vertically in a quiescent environment, and ignited at its lower end. To pass the test, it must extinguish within 150 mm propagation length. Even though PMMA does not pass this test, it is extensively used for scientific investigations because of its repeatability and use in previous studies. Systematic ground tests of generic geometries have revealed that almost any realistic machined geometry like sharp or rounded edges, fins or grooves may lead to a rise in flame propagation velocity up to a factor of four related to the flat standard sample. For the first time, the flamed spread over a structured, thick PMMA sample of 290 x 50 mm was examined in microgravity ($3x10^{-5}g_0$) under concurrent flow of 0.20 m/s onboard Orbital ATK's re-supply spacecraft Cygnus. The results were compared to the behavior of a similarly-sized flat sample. Just as in 1g, it was found that vertical structures promote faster flame spread compared to a flat sample but to a lesser degree than what is observed in 1g. While the structured sample burned 70% faster than the flat sample in 1g, this difference was reduced to only 32% in microgravity. Both samples burned drastically slower in microgravity: 23 times slower for the structured sample and 18 times slower for the flat sample. In 1g the pyrolysis front rapidly spreads along the surface and takes advantage of improved in depth heat transfer afforded by edges but, in microgravity, the burning mostly confined to the leading edge which has the best supply of oxygen. Finally, the microgravity flames produced more smoke and exhibited a larger preheat area.

[1] Head of Combustion Engineering Working Group, ZARM University of Bremen, Am Fallturm, 28359 Bremen.
[2] Combustion Research Working Group, ZARM University of Bremen, Am Fallturm, D-28359 Bremen.
[3] Branch Chief, Combustion and Reacting Systems Branch, 21000 Brookpark Road, MS 77-5, Cleveland, OH 44135.
[4] Physical Scientist, Space Technology Office, 21000 Brookpark Road, OH 44135, MS 77-7, Cleveland, OH OH 44135.
[5] Spacecraft Fire Safety Researcher, 21000 Brookpark Road, OH 44135, MS 77-5, Cleveland, OH 44135.
[6] Staff Scientist, USRA, 21000 Brookpark Road, MS 110-3 Cleveland, OH 44135.
[7] Chair of BRE Centre for Fire Safety Engineering, University of Edinburgh, EH9 3FB, UK.
[8] ESA/ESTEC, Keplerlaan, 2201 Noordwijk, The Netherlands.

Nomenclature

SAFFIRE = Spacecraft Fire Safety Demonstration
PMMA = Polymethyl methacrylate (Plexiglass©)
ISO = International Organization for Standardization
ITT = International Topical Team
SIBAL = Cloth of 25% glass fibre and 75% cotton

I. Introduction

ALL the materials used in habitable spacecraft including internal structures, experiments racks, thermal and electrical insulation, fabric, containers, equipment and consumables must pass a standard flammability test (NASA STD 6001B[1]). This test was intended to provide a conservative measure of a materials´s flammability and has been used for decades to improve spacecraft fire safety.

Part of this standard is the upward flame propagation test (*Test 1*). Its purpose is to determine if a material, when exposed to an ignition source, will self-extinguish and not transfer burning debris, which can ignite adjacent materials. In *Test 1* a material sample with the dimensions 300 mm by 65 mm, and with a thickness as foreseen for use, is mounted vertically in a test frame in a 1g laboratory environment. The samples must be flat and the sample edges need to be protected from burning. The entire assembly is mounted in a chamber to protect the combustion process from outer air motion and the atmosphere must represent the worst-case to which the material could be exposed. The size of the cabinet must be designed to ensure that the oxygen concentration does not drop by more than 5% (rel.) during burning. The sample is then ignited at its lower end and is deselected when it does not self-extinguish within an upward propagation length of 150 mm and/or when it expels burning debris. Materials that do not pass *Test 1* can still be used through a waiver process, if no alternative material can be found and if appropriate configuration controls are applied.

Even though the selection criteria seem to be somewhat arbitrary they have been empirically modified, improved and adopted to new technical materials over the years. The NASA standard was taken over by ESA and transferred into an ECSS standard[2] and then eventually into an international ISO standard[3]. But the predominant problem with characterizing materials flammability for space application through ground based experiments remains, namely that burning in microgravity proceeds differently than in normal gravity in almost all relevant aspects. As will be demonstrated later, in 1g conditions the heat flux from a flame propagating in a buoyant flow into the sample is not only higher but is also stretched over a larger area due to buoyancy. In some cases, the buoyant flow speed becomes so large that the base of the flame is "blown off," destabilizing the flame and leading to extinction. By eliminating buoyancy and imposing a forced flow speed less than the induced buoyant flow which caused blow-off it may be possible for the flame to be sustained. This might lead to a situation where a flame may not propagate in 1g (material passes *Test 1*) but would propagate in µg. The simple "pass" or "fail" approach might therefore be appropriate within one domain (1g or µg) but a transfer of a threshold propagation length from the one into the other domain is disputable. Unfortunately, the database to compare ground based behavior to the behavior of the same material in space is rather sparse. The main reason is that flame spread experiments with realistic solid fuels require long test durations. Drop tower and parabolic f light experiments are meaningful only for thermally thin fuels (sheets or wire insulation) or for ignition investigations. Sounding rocket offers some improvement with several minutes of test time available, but these come at a significant cost increase. The accessibility to long duration facilities required for thick fuel experiments is very limited. These environments are manned, and so safety concerns limit the size and scope of combustion experiments. Small samples often suffer from boundary effects through sample edges or sample holders or interactions with the narrow confinement. Last, but not least, such flame spread experiments are costly and require large amounts of oxidizer, which in turn makes comprehensive parametric studies difficult. Therefore, many questions remain open and there is a strong impetus to relate microgravity combustion behavior to scientific fundamentals rather than to rare experiences and sparse empirical data in order to gain a deepened understanding on how flame spread over solid materials is altered in microgravity. Initiated through NASA, the SAFFIRE science team has thus planned to perform a number of carefully selected experiments within the "Spacecraft Fire Safety Demonstration Project"[4-6]. This represents a very valuable and rare opportunity. The research program is based on the utilization of the uncrewed resupply spacecraft Cygnus for large scale fire safety experiments after it had accomplished its mission. A series of six subsequent flights will be used to investigate materials flammability and flame propagation in normal air as well as under normoxic conditions of enhanced oxygen concentration and reduced pressure as foreseen for future exploration missions. Results of the second flight of the series are presented and discussed here.

When building a spacecraft, there are many materials to choose from but the number of truly non-flammable materials (e.g. ceramics) is quite small. Whenever flammable materials are used, absolute safety is not achievable. In order to improve fire safety it is important to understand how the risk changes with respect to relevant parameters including ignition source and ignitability, thermal properties, composition of exhaust gases and materials shape or constitution in case of compound materials.

The latter was subject of the experiments onboard the ISS resupply spacecraft Cygnus within this SAFFIRE II experiment. Investigations on the effect of surface structures on flame spreading were very limited so far. For the thermally thin material, Nastac and T´ien[7] examined the upward propagation of the flame on linerboard and cardboard with horizontal and vertical corrugations. They found that vertical sinusoidal corrugations promote spreading more than horizontal corrugations and that for both cases the flame propagation is enhanced compared to linerboard. The experiments were performed only in 1g conditions. Similar configurations were numerically simulated by Stalcup[8] and qualitatively compared to the experiments of Nastac and T'ien. Stalcup found that the larger the amplitude of the corrugations, the larger the growth rate, because the flame only heats the crests losing little heat to the valleys. Similarly, the burnout rate decreased as the lower heat transfer to the valleys reduces the preheating there leading to a slower propagation of the flame base. With larger corrugations he also found that the initial growth of the heat release rate is quicker and reaches higher peak values. Furthermore, a number of studies were performed in 1g to systematically examine the effect of surface-structured, thermally thick PMMA[9-14]. Meyer[15] developed an empirical model describing the effect of structures on the propagation velocity and the effect of structure interactions for the 1g case. This model allowed for rather accurate predictions, but could not be applied to microgravity conditions. This is attributed to the differences in combustion and its interactions with the flow-field.

II. Experimental Setup

The experimental rig, as shown in Figure 1, was installed into the Cygnus cargo bay. It consists of a large flow duct measuring 460 x 510 mm cross section. The flow duct was split along the center line by the sample holder, which contained nine samples that were burned sequentially starting with the most downstream sample. Samples 8 and 9 were the PMMA samples and thus the last to be ignited. Both samples were 290 mm long and 50 mm wide. The samples were allowed to burn on both sides and, in case of the structured sample, both sides were identically shaped.

Figure 2 depicts the cross sections of samples 8 and 9. Sample 9 was flat and unstructured and thus served as a reference test assimilating the *Test 1* requirements. Sample 8 had grooves with different patterns along which different propagation velocities were expected. Both samples were tapered towards on the leading and trailing edges, as shown in Figure 3. The upstream taper was manufactured with a line of holes through which a 29 gage Kanthal© resistance wire was coiled for ignition purposes. The igniter was powered for 30 s after the air flow was established. The downstream taper of the same dimensions served to straighten the air flow in order to influence the incoming flow to the downstream samples as little as possible.

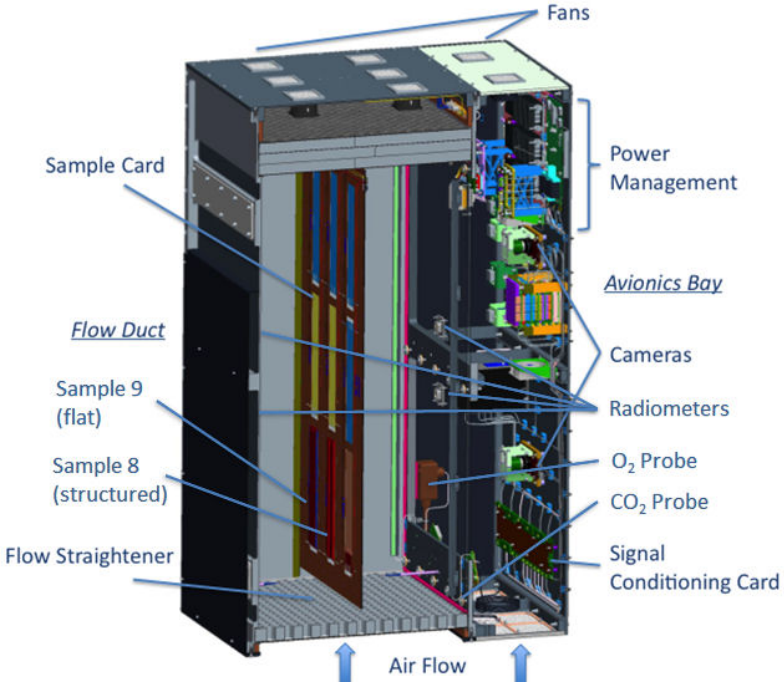

Figure 1. Experimental setup

The air flow was drawn through the duct by fans located at the downstream end. The duct entrance contained a flow straightener. At the exit, filters collect particulate combustion products to prevent them from reentering the chamber. The whole cargo bay of the

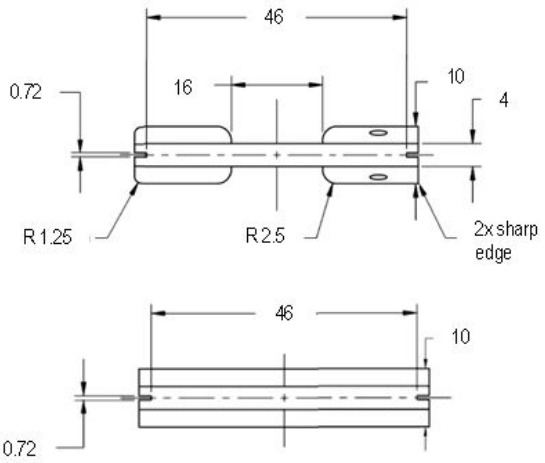

Figure 2. PMMA samples 8 (top) and 9 (bottom)

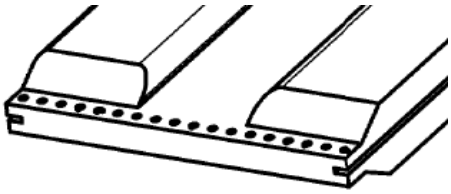

Figure 3. Tapered upstream (igniter) end

Cygnus spacecraft served as air reservoir for the experiments. Two high resolution cameras were used to observe the samples during the experiment, one of which was looking towards samples 8 and 9. The frame rate was set to 30 f/s. The image files were transferred to ground first in jpeg compression format. Selected images or image sequences were then downloaded in raw format. Every two seconds, a green LED was switched on for 0.5 s to illuminate the pyrolysis front. Unfortunately, the flame for the PMMA samples was so bright that it dominated the camera´s exposure setting and the green lighting was rendered inadequate for illuminating the samples surface. The pyrolysis front could only be observed after extinguishment of the sample.

The burning process was also monitored by four radiometers, two on each side of the sample. The main purpose of the radiometers was to determine if burning proceeded symmetrically on both sides of the holder card.

Two anemometers, one on each side, measured the air flow velocity and adjusted the rpm of the fans to maintain a flow velocity of 0.20 m/s. This velocity was chosen to coincide with the average velocity of the ISS´s air conditioning system. An O_2 sensor measured the incoming oxygen concentration, which was expected to drop slightly during the experiments from the initial value of 22.1 %. In parallel, a CO_2 sensor monitored the accumulation of exhaust products in the incoming air.

Sample 8 was extinguished by switching off the air flow 10 min after ignition, while sample 9 was extinguished by the same method after 15 min. The flow through the avionics bay which contained the gas probes was kept on throughout the whole experiment duration.

For comparison, the 1g experiments were performed in a closed chamber according NASA STD-6001B. Instead of a camera operating in the visual range, a FLIR Tau2© 640 IR-camera was used. This camera allowed a look through the flame in order to follow the damage front on the sample´s surface over time. After defining the temperature of the damage front to coincide with 330 °C, an automatic software routine followed the 330 °C line over time. The sample was extinguished when the foremost pyrolysis front reached the upper end of the sample. The sample was weighed before ignition and after extinction to measure the average mass burning rate.

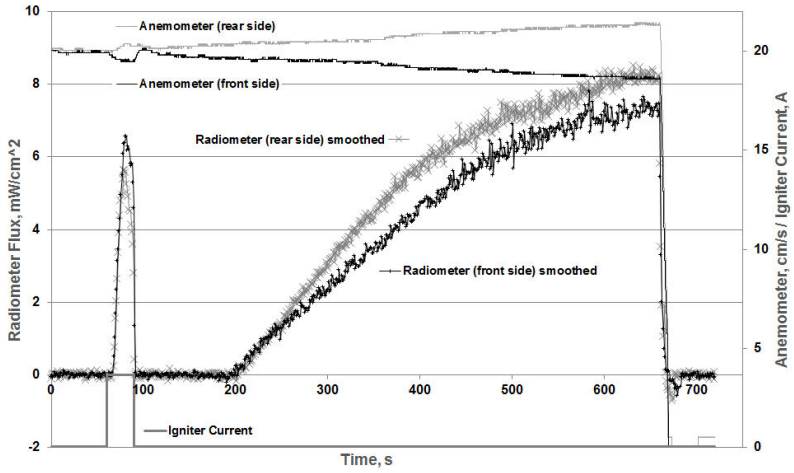

Figure 4. Sample 8, readings of the radiometer and anemometer

III. Results and Discussion

A. Methods of Data Evaluation

The intended conditions as described in section II were not fully matched. During the burning of sample 8, the average flow velocity remained at the intended value of 0.20 m/s, but the velocity on the observation side of the card dropped to 0.186 m/s in continuous increments while the flow velocity on the rear side increased accordingly to 0.214 m/s. As a result, the radiometer readings did not show the same flame intensity on both sides with the flame being brighter on the side with the higher velocity (rear side)

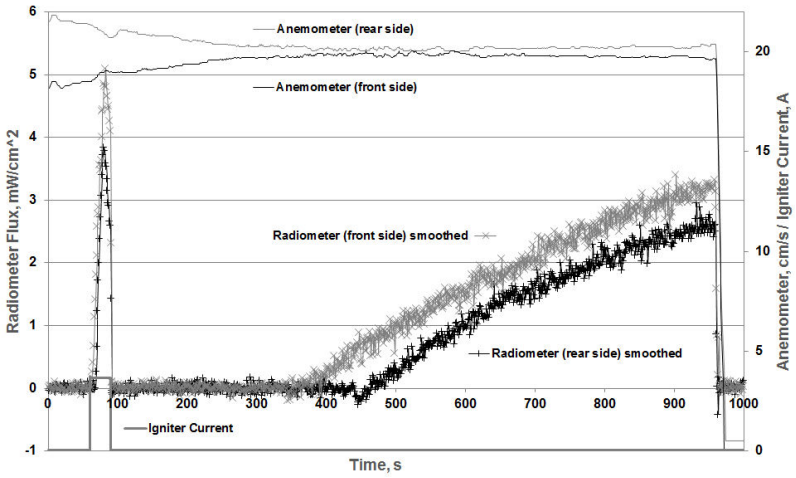

Figure 5. Sample 9, readings of the radiometer and anemometer

as shown in Figure 4.

When switching the air flow on again for sample 9, the flow velocities remained split at first but the difference decreased to less than 0.01 m/s after approximately 400 s. Again, the radiometer reading on the rear side was stronger than on the front side (Figure 5). The reason for this deviation has not yet been determined. Also, the output of the oxygen sensor was questionable during this experiment and could not be used for evaluation.

Some differences between the behaviors of samples 8 and 9 are remarkable. The start of the rise of the radiometer reading happens after quite different periods of no signal after ignition, even though the power applied to and the geometry of the igniter wires for the two samples were identical. The front side video revealed that sample 9 appeared to be practically extinguished after ignition and it took quite a long time until the flame recovered or was re-ignited by the flame on the rear side of the leading edge as the difference in the rising point of approximately 100 s suggests.

Another difference is regarding the different intensities of the radiation during ignition. Again, the ignition conditions must have been mostly identical. The maximum radiometer readings are 6.5 mW/cm^2 on the front side of sample 8 and only 5.1 mW/cm^2 on the rear side of sample 9. The differences between the front and the rear side can be explained by the differences in the flow velocities that provoke a brighter flame. The differences in the maxima during ignition can be easily attributed to the slightly larger view angle of sample 9 to the radiometer as the angular sensitivity of the radiometer is strong.

While the maximum radiometer value of sample 8 indicates that steady state was almost achieved, the very long period the flame of sample 9 needed to develop is responsible for not achieving steady state even after 15 min. The relative difference in the maximum reading is again attributed to the extreme position of the sample relative to the radiometer. However the lower level of the sample 9 maximum radiometer reading relative to the level during ignition indicates the lower intensity of the flame compared to sample 8.

In order to determine the propagation length of the pyrolysis front during burning, it is important to define the moment from which the flame is fully established and starts propagating. The radiometer readings seem to make this point easy to determine (195 s for sample 8; 450 s for sample 9). A closer look at the sensitivity curve of the radiometer and comparing these readings to the visual appearance suggests that the moment from which the flame is fully established is quite some time sooner than the radiometer indicates. In Figure 6 we can see that the CO_2 signal starts to rise sooner than the radiometer. This even though, the CO_2 probe is located as the entrance side of the avionics bay (see Figure 1) and can detect the CO_2 rise only after the exhaust gas has passed through the Cygnus cargo bay before it re-enters the experiment container. Figure 6 also shows the strong noise on the radiometer signal which is smoothed by applying a low pass filter in Figure 4 and Figure 5. During burning, this "noise" is slightly augmented by frequently occurring jets of pyrolysis gas penetrating the flame zone into the oxygen-rich flow above the flame as explained later. Thus, it appears reasonable that the radiometers sensitivity is not high enough to be used

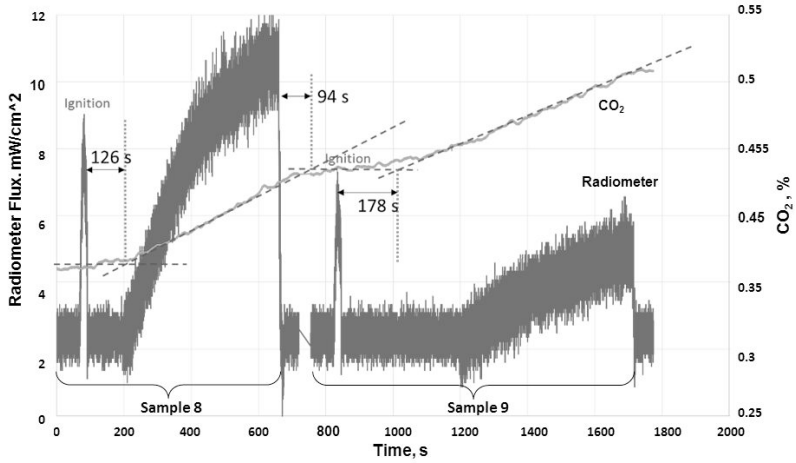

Figure 6. Front side radiometer and CO_2 Sensor readings during burning of sample 8 and 9.

to determine the starting point. When backward extrapolating the slope of the CO_2 sensor signal during steady burning to a horizontal line at the concentration during ignition, the starting point is essentially earlier. Looking into the respective flame images reveals that there is a weak, but fully developed flame that is not significantly different in the seconds before and after. As such, there was no other more objective way than looking through the individual images and to decide for the moment when the flame has developed over the full width of the sample. *This moment was 14 s after the ignition ended for sample 8 and 100 s after the ignition ended for sample 9*. This selection seems to be reasonable when looking at the lag of the CO_2 signal of 94 s after sample 8 was extinguished. Subtracting this lag from the delay of 126 s until the CO_2 signal rises and 178 s for sample 9 we get 32 s for sample 8 and 84 s for sample 9, which is in the same range. The steady burning time of sample 8 was thus 555 s from being fully established until extinction, while sample 9 burned for 770 s.

B. Flame Propagation Velocity

Figure 7 depicts samples 8 and 9. Figure a) through d) shows the samples immediately after extinction. In figure b) it is overlain with the flame´s appearance right before extinction. In figure c) the pyrolysis front at the end of the burning period is marked in red and the burnout end is marked in yellow. In figure d) the samples are overlain with the fringes that follow the pyrolysis front through IR-videography during 1g experiments. The distance between each fringe is 30 s. Figure e) shows the shape of the burnout end of the samples burnt in 1g-conditions. All images are truncated to the same length. Therefore the most upward extent of the pyrolysis front of the 1g samples is cropped.

From these images the following quantitative results were obtained and are summarized in Table 1. As can be clearly seen, the propagation length is generally much smaller in microgravity than in 1g. For sample 9, the flames at the outer edges lag behind while in the 1g experiment they are ahead. The reason for this is that sample 9 was

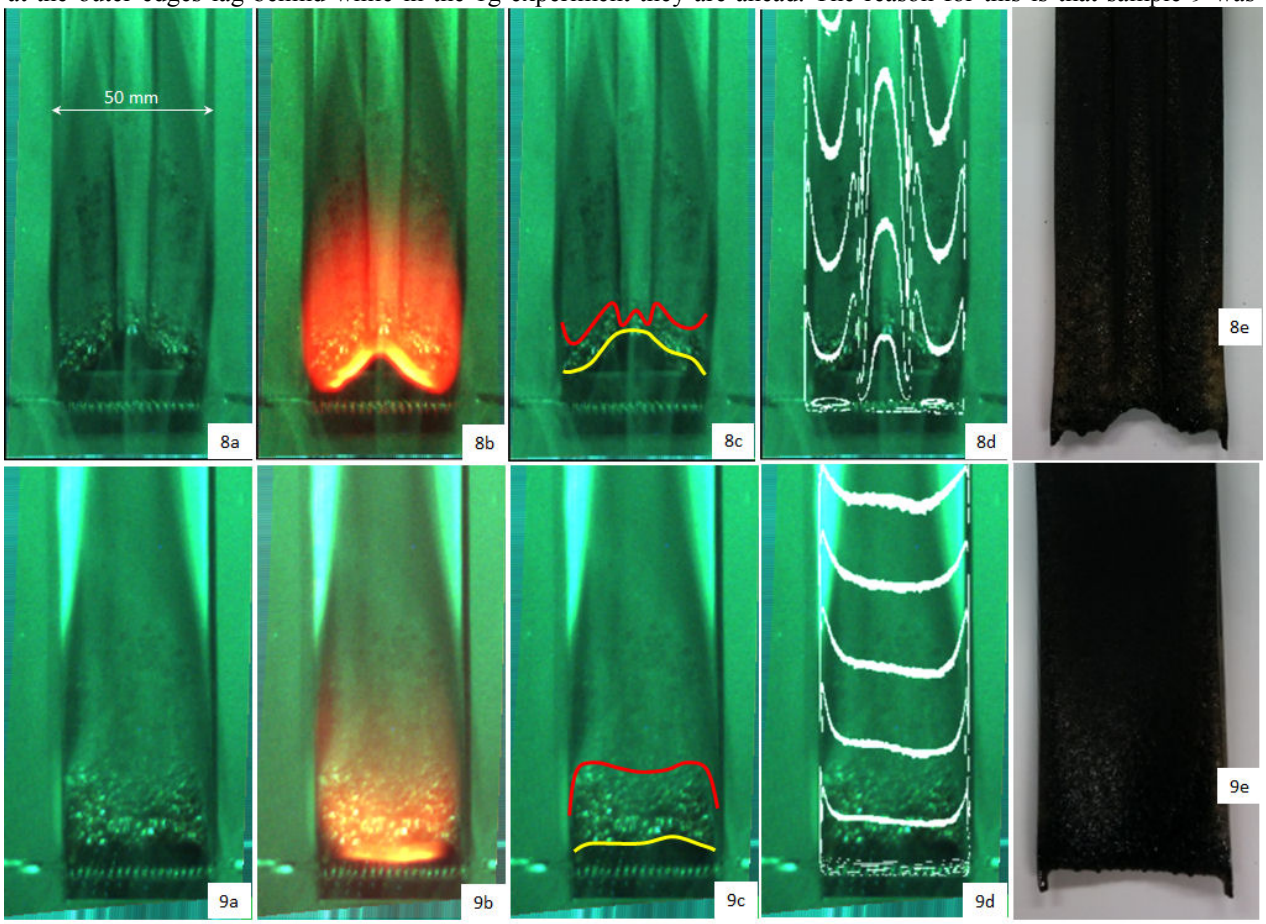

Figure 7. Samples 8 (top) and 9 (bottom). a) immediately after extinction, b) overlain by the flame immediately before extinction, c) pyrolysis front (red) and burnout end (yellow), d) samples overlain by the pyrolysis fronts detected in 1g through IR videography (time between fringes = 30 s), e) burnout end of the 1g samples.

Table 1. Comparison of Results. The error in measured values d and l is ± 0.5 mm.

	Sample 8		Sample 9	
	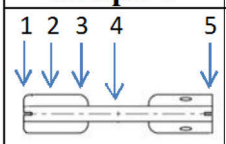		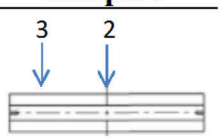	
	SAFFIRE II	1g	SAFFIRE II	1g
Burn duration, s	555	120	770	210
Propagation distance, mm				
d1	29	157		
d2	22	133	35	184
d3	36	185	38	192
d4	34	175		
d5	32	153		
Pyrolysis front velocity, mm/s				
pv1	0.05	1.31		
pv2	0.04	1.11	0.05	0.88
pv3	0.06	1.54	0.05	0.91
pv4	0.06	1.46		
pv5	0.06	1.28		
Burnout length, mm				
l1	12	0		
l2	18	4		
l4	26	10		
$l_{average}$			11	6
Burnout velocity, mm/s				
bv1	0.02	0.00		
bv2	0.03	0.03		
bv4	0.05	0.08		
$bv_{average}$			0.01	0.03

equipped with vertical aluminum sheets along the outer sides removing heat along the edges of the sample while in the 1g experiment, as well as with sample 8, the sample was only held in the slit along the center axis of the samples sides by a horizontal aluminum frame. As the propagation front of sample 9 shows a plateau in the central area it is evident that this drag down on the edges does not affect the maximum propagation velocity in the central region.

A comparison of the differences between the samples compare in 1g and µg-conditions is more interesting. The 1g data are based on experiments on five identical samples. The spread at all edges was less than 2%. In µg only a single sample could be processed. However, as the spread in 1g was so small, it is beyond doubt, that the µg result is a reliable representation of the µg behavior. The pyrolysis front velocity is calculated by division of the measured lengths through the related burn duration. While the maximum pyrolysis front velocity along the structured sample is 70% faster than on the flat sample in 1g, this difference is reduced to only 32% in microgravity. The structured sample itself burns 23 times slower in microgravity while the flat sample is only 18 times slower. Assumed the temperatures of the diffusion flames are comparable in 1 and µg, the gas density through the flame drops for about a factor of 7. This leads in 1g as well as in µg to a thickening of the reacting layer but additionally in 1g to upward velocity gradients in the same order. These gradients are assumed to introduce vorticity in this shear layer supporting the gas exchange in the direction normal to the sample´s surface. As this transport parameter is missing, in microgravity the reaction zone remains mostly layered with only small velocity differences through the flame. Thus, the flame zone is well and comparably ventilated only at the leading edge and is very fuel rich further downstream. That the leading edge is sufficiently provided with oxygen is also supported by the fact that the burnout end of both samples has a very similar shape in 1g and in µg and that the propagation velocity of the burnout end is only reduced by a factor of two for both samples. However, the burnout end in the groove (4 mm thick) propagated 3 times faster than at the flat sample (10 mm thick).

Another important indication for the different mechanisms in the propagation velocity of the pyrolysis front between 1g and µg is regarding the observed flame length. While in 1g the flame length increases rapidly with time, it achieves an almost constant length in microgravity. For a given fuel this length is assumed to mainly depend on the velocity of the incoming air flow. The rationale is rather simple - due to the shear-layer induced vorticity in 1g, any pyrolysis gas ejected from the surface will be burned with entrained oxygen. Thus, the vaporizing area can expand with time and so does the flame. This relation also explains why the flame propagates faster along structures adjunctive to volumes with smaller heat capacity and accordingly larger local heating rate in 1g. In µg the local heating rate along structure edges remains higher and also the pyrolysis rate remains increased there, but due to the fact that the gas exchange normal to the sample is reduced, this increased pyrolysis stream due to an increased heating does not contribute to propagation as most of it is not burnt but contributes to increased smoke emissions. In

the unperturbed layer in µg the length of the pyrolysis zone that contributes to combustion depends only on the local gas exchange due to diffusion. The flame length then depends on reaction kinetics and on the flow velocity to stretch the reacting layer. This explains why the large difference in propagation velocity in 1g diminishes in µg.

However, like in 1g, the edges along the structured sample remain the zones with the fastest spreading rates. Even though the structures are such close on the narrow sample that they must interfere with each other, differences of 30% over the sample´s width in spreading rate remain.

For both samples, it can be asserted that due to the reduced ventilation in microgravity, the fire tends to penetrate more into the material´s depth rather than to spread along the surface as in 1g. While a fire in 1g might become evident to a detection source by its radiation from a widespread area before a serious damage in the depth occurs, in µg a fire can cause damage to the material in depth (or to the material behind the combustible) long before it is detected.

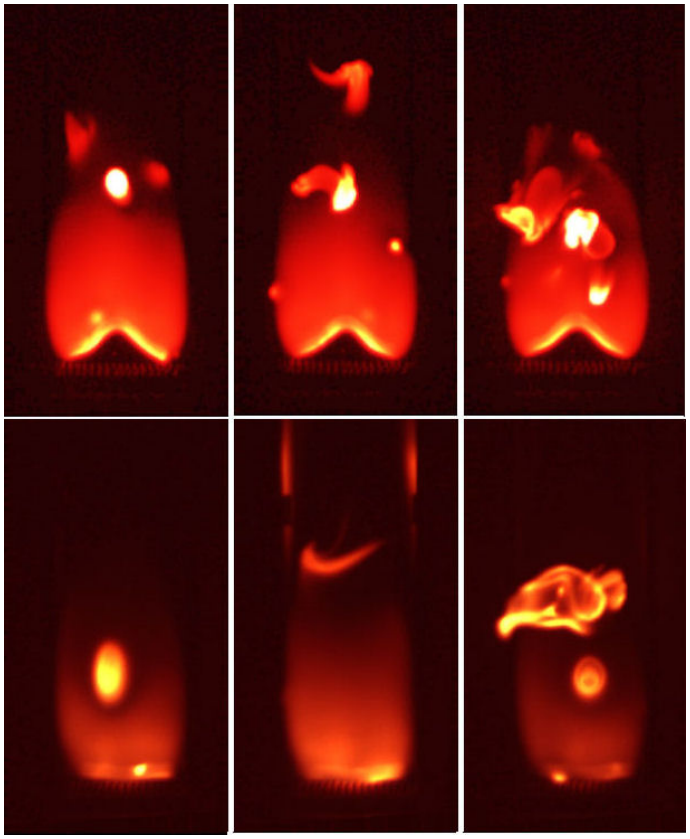

Figure 8. Examples for frequently occurring jets from flammable pyrolysis gas bubbles ejected through the oxygen depleted zone into the fresh air above the flame. Sample 8 (top), sample 9 (bottom).

Another difference that was observed was for smoke. The results indicate that the preheated area underneath the flame is even larger than in 1g. This is derived from two observations. First, the area in front of the pyrolysis front shows the slight bubble craters in the after burning image are longer than in 1g. Secondly, one can frequently observe large jets deriving mostly from ahead of the flame base. This occurred for both samples as also shown in Figure 8. This is assumed to attribute to the strong preheating ahead of the flame base that causes the release of flammable pyrolysis gases. As the sample´s local heating rate was larger around the edges and in the groove of sample 8, these events occurred more frequently and stronger as with sample 9. This can also be deduced from Figure 6 where the radiometer signal´s "noise" due to such light flickering increased with time with sample 8 but remained mostly constant with sample 9. In case of a low momentum of the jets, the gases are removed towards downstream underneath or inside the flame zone without being burnt due to the lack of oxygen until they reach a zone where oxygen from the unperturbed flow is entrained. However, at that point, the temperature is already too low to ignite the vapors. Ignition and combustion events initiating ahead of the luminous zone have never been observed. In case the ejection momentum is high, the jets may penetrate the flame zone into the oxygen-rich layer above the flame and burn there. While the latter is observed (Figure 8) there is no proof for the former. But it is not at all reasonable that any gas jet from the samples surface must have enough momentum to achieve a sufficient penetration height to reach the oxygen rich layer. In contrast an impulse distribution must be assumed. This is an important difference to the 1g-case where nearly all of the pyrolysis gas is burnt and the combustion of PMMA produces only small amounts of smoke. In microgravity, there must be a higher production of flammable gases and particulates that exit the flame zone without being burnt. This must then have an impact on the development of fire-fighting strategies where in this case there is the constant hazard of inducing flash-over events when disturbing the boundary layer of the flame zone.

IV. Conclusion

Two PMMA samples were burnt in concurrent flow of normal air and 0.20 m/s flow velocity in 1g and in microgravity onboard the Cygnus re-supply spacecraft. One sample had surface structures parallel to the flow

direction the other was flat. In contrast to 1g, where the flame and the pyrolysis area become longer with progressing combustion, the flames in microgravity achieved a mostly constant and comparably short length. This is attributed to the finding that the flame is limited to a narrow area around the leading edge in microgravity. This is assumed to be the only area that is sufficiently supplied with oxygen. Further downstream the flame still heats up the subjacent material and induced pyrolysis (more at the sharp structures with small heat capacity) but it also shields this material against oxygen. While in 1g the pyrolysis front propagates 70% faster along the edges of the central groove compared to the flat sample, this difference is reduced to only 32% in microgravity. Both samples burn significantly slower in microgravity: 23 times slower for the structured sample and 18 times slower for the flat sample. As the preheat area is larger in microgravity, both samples produce more smoke of unburnt gas and particulates in microgravity. Even though the propagation velocity of the pyrolysis front along edges and grooves is significantly smaller in microgravity, a difference +32% compared to an unstructured surface remains. Structures in the surface mainly affect the area close to the flame base. The sharper the edges of a contour at the flame base are, the better is the combustion supported in the way that the combustion heat transfer in-depth is higher at edges. With this it appears reasonable that structuring may support self-sustained burning of a material that extinguishes in flat configuration. Structured or not, the microgravity combustion produces more smoke and thus flammable but unburnt gases and particulates compared to 1g. This imposes the hazard of flash-over combustion when disturbing the boundary layer and air is actively entrained into the layered system, for example when initiating fire-fighting activities.

Given there were the chance for complementary experiments in µg or just to repeat the experiment, the additional installation of an IR-camera were desirable. Such a camera was applied to the 1g-experiments and did not only allow to directly depict the pyrolysis front as the camera can look through the luminous flame directly onto the sample´s surface, also the samples temperatures could be measured rather accurately. A quantitative comparison of the materials temperature during 1g- and µg-experiments could deliver additional valuable data. These data at hand it is conceivable that the empirical model developed by Meyer et al.[15] predicting the shape dependent burning behavior of PMMA for 1g conditions could also be applied µg conditions.

Acknowledgment

The authors thank NASA for the provision of this outstanding opportunity and for its financial support. The support from the topical team on fire safety in space (ESA-ESTEC contract number 4000103397) is also appreciated.

References

[1]NASA, "NASA-STD-6001B, Flammability, Offgassing and Compatibility Requirements and Test Procedures", NASA, 2016.
[2]ECSS, 5. February 2010, "ECSS-Q-ST-70-21-C", ESA Requirements and Standards Division, 2010.
[3]ISO, "ISO 14624-1A Space systems — Safety and compatibility of materials — Part 1: Determination of upward flammability of materials", 2008.
[4]Ruff, G. A. and Urban, D. L., "Demonstration of Spacecraft Fire Safety Technology", *42nd International Conference on Environmental Systems (ICES)*, 2012-3510-San Diego, CA, 2012, 8.
[5]Urban, D. L., Ruff, G.A., Minster, O., Fernandez-Pello, A.C., T´ien, J.S., Torero, J.L., Legros, G., Eigenbrod, C., Smirnov, N., Fujita, O., Cowlard, A., Rouvereau, S., Toth, B., Jomaas, G., "Unmanned Vehicle Material Flammability Test", *28th meeting of the American Society for Space and Gravitational Research*, New Orleans, LA, 2012, .
[6]Joomas, G., et al., "Fire safety in space – beyond flammability testing of small samples", *Acta Astronautica,* 109-2015, 2015, 8.
[7]Nastac, G. C. and and T´ien, J., "The Effects of Corrugation on Thin Solid Fuel Upward Flame Spread", *Case Western Reserve University*, 2014-EMAE 398, Cleveland, OH, 2014, 15.
[8]Stalcup, E. J., "Numerical Modeling of Upward Flame Spread and Burning of Wavy Thin Solids", Case Western Reserve University, M.Sc., Cleveland, OH, 2015, 171.
[9]Freier, A., "Upward Flame Propagation Test (NASA-STD 6001): Investigation of the interaction between surface-structures and flame propagation", University of Bremen, B.Sc., Bremen, 2014, 55.
[10]Meyer, F., "Generation of a numerical model to simulate the radiative heat transfer onto a surface-structured material sample including execution and evaluation of parametric studies", University of Bremen, B.Sc., Bremen, 2013, 64.
[11]Nordmann, C., "Comparative Investigations on the Flame-Propagation along differently surface-structured Samples", Universität Bremen, B.Sc., 2013, 65.
[12]Schwenteck, T., "Experimental Investigation of the Flame-Propagation along Surface-Structured PMMA-Samples", University of Bremen, B.Sc., Bremen, 2014, 66.
[13]Stein, A. B., "Upward Flame Propagation Test (NASA-STD 6001): Experimental investigation of the flame propagation along cylindrical PMMA-Samples", Universität Bremen, B.Sc., Universität Bremen, 2015, 1-50.

[14]Würzburg, N., "Experiments on the vertical fame propagation along surface-structured PMMA-samples; Influence of sample thickness", Universität Bremen, B.Sc., Universität Bremen, 2015, 1-60.
[15]Meyer, F., Schwenteck, T., Ruhe, M., Bihn, P., Freier, A. and Eigenbrod, C., "UB-FIRE Experiment Results on Upward Flame Propagation along Cylindrical PMMA Samples in Reduced Gravity", *47th ICES*, 2017-98, Charleston, SC, 2017, 11.